CHARACTERISTICS OF CHIRAL BANDHEAD

V. Kumar†, A. Shukla, Manoj Kumar Sharma, P.K. Rath

Department of Physics, University of Lucknow, Uttar Pradesh 226007, India

Received 12 November 2022, accepted 3 January 2023, published online 17 January 2023

The bandhead of most chiral bands are isomers with a large Weisskopf hindrance factor. Such isomers are proposed as a type of K isomer. From the data available for the mass region $A \backsim 80, 100, 130$, and 190, it has been observed that the low value of reduced hindrance factors could be indicative of triaxial shape and orthogonally coupling of the valence nucleon angular momentum at the chiral bandhead.

DOI:10.5506/APhysPolB.54.1-A1

1. Introduction

Nuclear chirality was originally suggested in 1997 in Ref. [1], and since then it has been investigated rigorously both theoretically and experimentally. The classic examples of chirality are triaxial odd–odd nuclei where the angular momenta of a high-j particle and a high-j hole are aligned along the short and long axis, respectively, and the angular momentum of collective rotation is aligned with the intermediate axis. Pairs of $\Delta I = 1$ doublet bands with the same parity and near degenerate energies have been observed in several odd–odd, odd–A, and even–even nuclei, in the mass region of $A \backsim 80$, 100, 130, and 190. Such doublet candidates have been observed in more than 30 nuclei. Several theoretical approaches have been employed to explain the observed doublet bands. For example, the particle rotor model (PRM) [1–5], the tilted axis cranking (TAC) model [6–10], the TAC plus random-phase approximation (RPA) [11], the collective Hamiltonian method [12, 13], the interacting boson-fermion fermion model [14], and the angular momentum projection (AMP) method [15–17]. The most successful approach has been made in terms of chirality in nuclear rotation by Dimitrov *et al.* [10].

Additional observables such as static quadrupole moment and g factor [18–22] can also characterize nuclear chirality. In nuclear physics, the g factor measurement provides essential data for the two odd-nucleon configuration assignment. The first measurement of the g factor (gyro-magnetic

† Corresponding author: vinod2.k2@gmail.com

ratio) in a chiral band has been carried out for the bandhead ($I = 9^+$, 56 ns) of ^{128}Cs [22]. The experimental g-factor value is $g = 0.59(1)$ and theoretically expected value is $g = 0.51$. This shows that the total spin ($I = 9^+$) of the isomeric state cannot be built chiefly by two angular momentum vectors of the odd nucleons. A significant core rotation component needs to be present in order to drive the g factor from $g = 0.51$ towards the experimental value $g = 0.59(1)$. The g factor can also be used to discern whether the three angular momentum vectors lie in a plane (planar configuration, known as chiral vibration) or whether they span the three dimensional space (aplanar configuration, known as static chirality).

One of the less addressed observations in the case of chirality is that the most chiral bandhead are isomers in nature. At present, there is no theoretical discussion to explain the isomer nature of chiral bandhead in the literature. In the present paper, we have addressed it and observed that the reduced hindrance factors are almost of the same order for the chiral bandhead in different mass regions. The low value of reduced hindrance factors is indicative of triaxial shape and orthogonally coupling of the valence nucleon angular momentum at the bandhead when nuclei exhibit chirality.

2. Hindrance factor and K isomer

The lifetime of a nuclear excited state that decays by γ-transition depends on the transition energy, ΔE, and the change in quantum numbers between the isomer and the state to which it decays, as following [23]:

$$\tau \propto \frac{1}{(\Delta E)^{2\lambda+1} \mid \langle f \mid T_\lambda \mid \rangle \mid^2},$$

where λ is the multipole order and T_λ is transition operator between the initial, i, and final, f, states. It depends on three factors, $\gamma-$transition energy, multipole order, and the underlying transition matrix element, which may be the product of many factors. If ΔE is small and the multipole order is large, the lifetime is likely to be relatively long. Weisskopf estimated the electromagnetic transition rates due to the transition of a single nucleon from an initial state to a final state; these estimates provide us with reasonable relative comparisons of the transition rates. The ratio of the experimental half-life, $t^{\gamma}_{1/2}$ to the Weisskopf estimate of the half-life of electromagnetic transition, $t^{w}_{1/2}$, is known as the Weisskopf hindrance factor [23–26], F_{W}

$$F_{\mathrm{W}} = \frac{t^{\gamma}_{1/2}(\text{experimental})}{t^{w}_{1/2}(\text{Weisskopf estimate})}.$$

If the observed decay rate of a certain γ-transition is several orders of magnitude smaller than the Weisskopf estimate, we might suspect that the

poor matching of the initial and final wave functions is slowing down the transition rate. Similarly, if the transition rate was much higher than the Weisskopf estimate, we can guess that more than one single nucleon is responsible for the transition.

The shell model predicts the existence of isomers when excited states require large multipole (λ) transitions for their decay. Nuclei with/or near the magic number are more or less spherical in their ground state. Moving towards the middle shell, the shape usually becomes deformed. At high angular momentum and high excitation energy, also the nuclei can change their shapes/deformations. It is known that most deformed nuclei preserve rotational symmetry and then, their states may be characterized by the K quantum number which is defined as the projection of the total angular momentum onto the symmetry axis. In most of the deformed nuclei, the transition probabilities depend on the difference between the K quantum numbers of the initial and final states, denoted by ΔK [26, 27]. If this difference is larger than the multipole order λ of the electromagnetic transition, then such a transition is hindered by the degree of forbiddenness (also known as K forbiddenness) given by $\nu = \Delta K - \lambda$. Here, it is more appropriate to utilize the role of the ν that further reduces to the $F_{\rm W}$, so-called reduced hindrance factor F_ν [28–30] and is expressed as

$$F_\nu = (F_{\rm W})^{1/\nu}\,, \tag{1}$$

$$\log F_\nu = \frac{1}{\nu}\log F_{\rm W}\,. \tag{2}$$

Such conditions can also occur when the gamma transition decays from a deformed level with K to the spherical level with zero K.

3. Systematics of chiral bandhead and discussion

To elaborate further, let us take the example of mass region $\sim$ 130 [31–35]. The observation of systematic chiral bands is built on unique-parity $h_{11/2}$ valence proton and neutron orbitals. From the Nilson diagram, one can see that the Fermi level lies in the lower part of the $h_{11/2}$ proton subshell (*i.e.*, $K = 1/2$), and the higher part of the $h_{11/2}$ neutron subshell (*i.e.*, $K = 11/2$). The angular momentum for an orbital with $K = 1/2$ is oriented along the short axis of the triaxial core, while for an orbital with $K = 11/2$ is oriented along the long axis [1, 36]. Such orientations result in a maximal overlap of the core wave function with the particle-like wave function and a minimal overlap with the hole-like wave function; in both cases, the overlap results in a decrease in energy due to the attractive nature of the nuclear force.

In such a scenario, the bandhead spin of chiral bandhead is generated mainly due to the mutually perpendicular angular momentum of quasiparticles. The bandhead spin can be calculated/expected with the help of Cosine law of vector addition *i.e.*, $\sqrt{j_\pi(j_\pi+1)+j_\nu(j_\nu+1)} \sim 8\hbar$ for $j_\pi = j_\nu = 11/2$, assuming no contribution from all paired nucleons of the core. Most of the chiral bands in the mass region ~ 130 have bandhead spin 8^+, which is reasonable with the calculation. Therefore, the bandhead spin for the $\pi h_{11/2} \otimes \nu h_{11/2}$ band itself suggests nearly orthogonal coupling of the angular momenta for the valence proton and neutron.

The chiral bandhead in mass region ~ 130 [31–35, 37–42], decaying by the E1 transition, which corresponds to the configuration change from $\pi h_{11/2} \otimes \nu h_{11/2}$ for the initial state into $\pi(d_{5/2}g_{7/2})\nu h_{11/2}$ for the final state [39, 40]. The $\pi h_{11/2} \rightarrow \pi(d_{5/2}g_{7/2})$ E1 transition is forbidden in spherical nuclei by the selection rules for the E1 operator, but in deformed nuclei, the $\pi h_{11/2}$ orbital picks up $f_{7/2}$ and $\pi h_{9/2}$ components, that allow for E1 transitions. Since these admixtures are necessarily small, the resulting E1 matrix element is small as well, which explains the relatively long lifetime.

In the present work, we have looked for the possibility of the chiral bandhead as a kind of K isomer. One can expect a correlation of the nuclear deformation/shape with the hindrances since *(i)* lower deformation implies higher rotational frequencies (for a given spin) and larger Coriolis effects, hence more K mixing in both initial and final states, and *(ii)* transitional nuclei where γ-softness effects could lead to a loss in the identity of K, essentially through mixing and, hence, that causes low hindrances [46]. Various studies by Walker and collaborators [47–51] examined the above characteristics *(i–ii)* in the mass $A \sim 130$, 180 and 250 regions. Also, the studies [51–53] showed strong correlations between the F_ν found and the product of the valence nucleon numbers, N_pN_n [54–56]. The N_pN_n reflects the characteristics of the deformation. One would expect a correlation with hindrance factors since at low values of N_pN_n, lower deformation implies higher rotational frequencies (for a given spin) and large Coriolis effects, hence more K mixing in both initial final states [46]. This leads to a low hindrance factor.

Here, it is proposed that the E1 transition, which emits from the initial state configuration $\pi h_{11/2} \otimes \nu h_{11/2}$ to the final state configuration $\pi(d_{5/2}g_{7/2})$ $\nu h_{11/2}$ occurs in mass $A \sim 130$ [39, 40]. The $\pi h_{11/2} \otimes \nu h_{11/2}$ orbitals are in deformed shape, while $\pi(d_{5/2}g_{7/2})$ is in a spherical shape. The K value for the deformed state can be calculated as $k_\pi + k_\nu \sim 6$ for $k_\pi = 1/2,\ k_\nu = 11/2$, while for the spherical state it is zero. The ΔK is 6 and ν would be 5 for E1 transitions. Similarly, for $\pi g_{9/2} \otimes \nu g_{9/2}$ and $\pi g_{9/2} \otimes \nu h_{11/2}$ configurations in mass $\sim 80, 100$ [43–45], where the deformed state decays into spherical a state and the ν values will be 4 and 5, respectively. The F_ν values are compiled in Table 1 for the E1 decay from the chiral bandhead isomer. For

Table 1. The $F_{\rm W}$ and F_ν values calculated for the E1 decay branches [38–45].

Isotopes	Configurations	I_γ	E_γ[keV]	$t_{1/2}$[ns]	ν	$F_{\rm W}$	$F_{\rm W}/10^4$	$F_\nu = (F_{\rm W})^{1/\nu}$
^{80}Br	$\pi g_{9/2} \otimes \nu g_{9/2}$	59 (1)	271.4	0.40	4	36007.82	3.60	13.77
^{100}Tc	$\pi g_{9/2} \otimes \nu h_{11/2}$	9 (2)	364.7	0.28	5	465020.20	46.50	13.59
^{104}Rh	$\pi g_{9/2} \otimes \nu h_{11/2}$	36 (1)	215.6	42	5	3744067.79	374.40	20.63
^{128}Cs	$\pi h_{11/2} \otimes \nu h_{11/2}$	100	158.7	50.00	5	776923.07	77.69	15.06
^{132}La	$\pi h_{11/2} \otimes \nu h_{11/2}$	27 (2)	350.8	0.10	5	59700.69	5.97	9.01
^{134}Pr	$\pi h_{11/2} \otimes \nu h_{11/2}$	100	306.5	3.18	5	347926.26	34.79	12.83
^{136}Pm	$\pi h_{11/2} \otimes \nu h_{11/2}$	100	42.7	1500.00	5	434782.60	43.47	13.41
^{138}Pm	$\pi h_{11/2} \otimes \nu h_{11/2}$	100	173.6	21.00	5	415151.51	41.51	13.29

consistency, only the E1 transitions are investigated here, similar to E2, $I \to I-2$ branch transitions used in Refs. [47, 57] to calculate F_ν values. Figure 1 shows the pattern of $F_{\rm W}$ and F_ν values. The $F_{\rm W}$ values seem to be randomly distributed, while the F_ν values appear to be uniformly distributed. This indicates a correlation between the $F_{\rm W}$ and F_ν values of chiral bands. Furthermore, the low value of F_ν for the chiral bands can be indicative of orthogonal coupling of angular momenta at bandhead and triaxial shape.

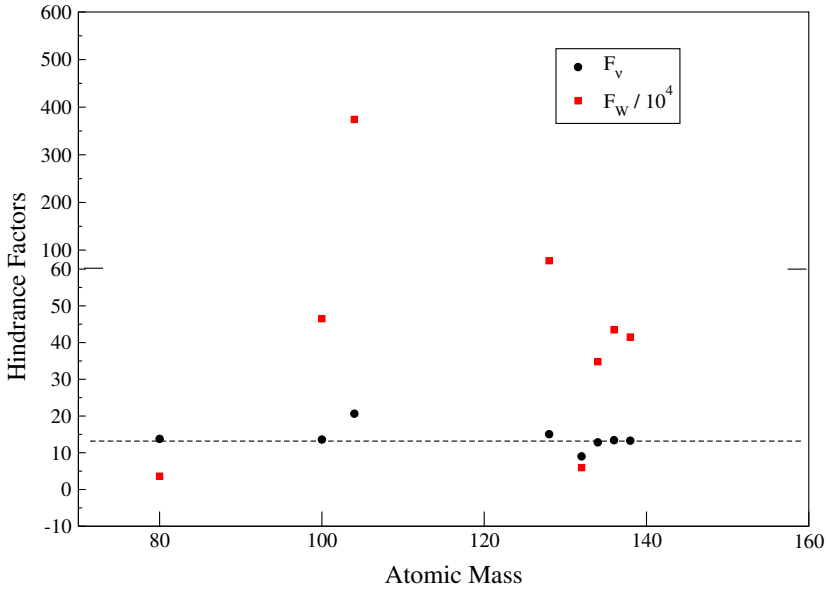

Fig. 1. Figure shows the comparison between $F_{\rm W}$ and F_ν values calculated for the E1 decay branches.

4. Conclusion

Most of the chiral bandheads show isomerism. Reduced hindrance factors from the E1 transition have been compared for chiral bandhead in mass ~ 80, 100, and 130 regions to explore a correlation between reduced hindrance factors and chiral bandheads. The low value of reduced hindrance factors is indicative of γ-soft/triaxial shape and orthogonally coupling of the angular momentum of valence nucleons at the chiral bandhead.

Financial assistance from the University Grant Commission (UGC) Start-Up grant and Inter-University Accelerator Centre (IUAC), New Delhi, is gratefully acknowledged.

REFERENCES

[1] S. Frauendorf, J. Meng, «Tilted rotation of triaxial nuclei», *Nucl. Phys. A* **617**, 131 (1997).

[2] S.Q. Zhang, B. Qi, S.Y. Wang, J. Meng, «Chiral bands for a quasi-proton and quasi-neutron coupled with a triaxial rotor», *Phys. Rev. C* **75**, 044307 (2007).

[3] B. Qi *et al.*, «Chirality in odd-A nucleus ^{135}Nd in particle rotor model», *Phys. Lett. B* **675**, 175 (2009).

[4] J. Peng, J. Meng, S.Q. Zhang, «Description of chiral doublets in $A \sim 130$ nuclei and the possible chiral doublets in $A \sim 100$ nuclei», *Phys. Rev. C* **68**, 044324 (2003).

[5] T. Koike, K. Starosta, I. Hamamoto, «Chiral Bands, Dynamical Spontaneous Symmetry Breaking, and the Selection Rule for Electromagnetic Transitions in the Chiral Geometry», *Phys. Rev. Lett.* **93**, 172502 (2004).

[6] P. Olbratowski, J. Dobaczewski, J. Dudek, W. Półciennik, «Critical Frequency in Nuclear Chiral Rotation», *Phys. Rev. Lett.* **93**, 052501 (2004).

[7] P. Olbratowski, J. Dobaczewski, J. Dudek, «Search for the Skyrme–Hartree–Fock solutions for chiral rotation in $N = 175$ isotones», *Phys. Rev. C* **73**, 054308 (2006).

[8] P.W. Zhao, «Multiple chirality in nuclear rotation: A microscopic view», *Phys. Lett. B* **773**, 1 (2017).

[9] D. Almehed, F. Dönau, S. Frauendorf, «Chiral vibrations in the $A = 135$ region», *Phys. Rev. C* **83**, 054308 (2011).

[10] V.I. Dimitrov, S. Frauendorf, F. Dönau, «Chirality of Nuclear Rotation», *Phys. Rev. Lett.* **84**, 5732 (2000).

[11] Q.B. Chen *et al.*, «Collective Hamiltonian for chiral modes», *Phys. Rev. C* **87**, 024314 (2013).

[12] Q.B. Chen *et al.*, «Two-dimensional collective Hamiltonian for chiral and wobbling modes», *Phys. Rev. C* **94**, 044301 (2016).

[13] S. Brant, D. Tonev, G. de Angelis, A. Ventura, «Dynamic chirality in the interacting boson fermion–fermion model», *Phys. Rev. C* **78**, 034301 (2008).

[14] F.Q. Chen *et al.*, «Chiral geometry in symmetry-restored states: Chiral doublet bands in ^{128}Cs», *Phys. Rev. C* **96**, 051303 (2017).

[15] G.H. Bhat, J.A. Sheikh, R. Palit, «Triaxial projected shell model study of chiral rotation in odd–odd nuclei», *Phys. Lett. B* **707**, 250 (2012).

[16] G.H. Bhat, R.N. Ali, J.A. Sheikh, R. Palit, «Investigation of doublet-bands in ^{124,126,130,132}Cs odd–odd nuclei using triaxial projected shell model approach», *Nucl. Phys. A* **922**, 150 (2014).

[17] M. Shimada, Y. Fujioka, S. Tagami, Y.R. Shimizu, «Rotational motion of triaxially deformed nuclei studied by the microscopic angular-momentum-projection method. II. Chiral doublet band», *Phys. Rev. C* **97**, 024319 (2018).

[18] Q.B. Chen, N. Kaiser, U.-G. Meißner, J. Meng, «Static quadrupole moments of nuclear chiral doublet bands», *Phys. Lett. B* **807**, 135568 (2020).

[19] Q.B. Chen *et al.*, «g factor and static quadrupole moment for the wobbling mode in ^{133}La», *Phys. Lett. B* **807**, 135596 (2020).

[20] C. Broocks *et al.*, «g-Factor and static quadrupole moment of ^{135}Pr, ^{105}Pd, and ^{187}Au in wobbling motion», *Eur. Phys. J. A* **57**, 161 (2021).

[21] E. Grodner *et al.*, «Examination of nuclear chirality with a magnetic moment measurement of the $I = 9$ isomeric state in ^{128}Cs», *Phys. Rev. C* **106**, 014318 (2022).

[22] E. Grodner *et al.*, «First Measurement of the Factor in the Chiral Band: The Case of the Isomeric State», *Phys. Rev. Lett.* **120**, 022502 (2018).

[23] G.D. Dracoulis, «Isomers, nuclear structure and spectroscopy», *Phys. Scr.* **T152**, 014015 (2013).

[24] P.M. Walker, F.R. Xu, «High- isomerism in rotational nuclei», *Phys. Scr.* **91**, 013010 (2016).

[25] V.F. Weisskopf, J.M. Blatt, «Theoretical Nuclear Physics», *John Wiley & Sons*, New York 1952.

[26] P.M. Walker, G.D. Dracoulis, «Energy traps in atomic nuclei», *Nature* **399**, 35 (1999).

[27] G. Alaga, K. Alder, A. Bohr, B.R. Mottelson, «Intensity Rules for Beta and Gamma Transitions to Nuclear Rotational States», *Kgl. Danske Videnskab. Selskab. Mat.-fys. Medd.* **29**, 9 (1955).

[28] C.J. Gallagher, «Classification of beta- and gamma-ray transitions between intrinsic states in deformed even-mass nuclei», *Nucl. Phys.* **16**, 215 (1960).

[29] K.E.G. Löbner, «Systematics of absolute transition probabilities of K-Forbidden gamma-ray transitions», *Phys. Lett. B* **26**, 369 (1968).

[30] L.I. Rusinov, «Nuclear Isomerism», *Uspekhi Fiz. Nauk.* **73**, 615 (1961) [*Sov. Phys. Usp.* **4**, 282 (1961)].

[31] K. Starosta *et al.*, «Chiral Doublet Structures in Odd–Odd Isotones: Chiral Vibrations», *Phys. Rev. Lett.* **86**, 971 (2001).

[32] K. Starosta *et al.*, «Role of chirality in angular momentum coupling for odd–odd triaxial nuclei: ^{132}La», *Phys. Rev. C* **65**, 044328 (2002).

[33] T. Koike *et al.*, «Observation of chiral doublet bands in odd–odd $N = 73$ isotones», *Phys. Rev. C* **63**, 061304 (2001).

[34] D.J. Hartley *et al.*, «Detailed spectroscopy of the chiral-twin candidate bands in ^{136}Pm», *Phys. Rev. C* **64**, 031304 (2001).

[35] A.A. Hecht *et al.*, «Evidence for chiral symmetry breaking in ^{136}Pm and ^{138}Eu», *Phys. Rev. C* **63**, 051302 (2001).

[36] J. Meyer-ter-Vehn, «Collective model description of transitional odd-A nuclei: (II). Comparison with unique parity states of nuclei in the $A = 135$ and $A = 190$ mass regions», *Nucl. Phys. A* **249**, 141 (1975).

[37] V. Kumar *et al.*, «Decoupling behavior in ^{132}La», *Phys. Rev. C* **82**, 054302 (2010).

[38] E.S. Paul *et al.*, «Rotational bands in doubly odd ^{128}Cs», *Phys. Rev. C* **40**, 619 (1989).

[39] V. Kumar, P. Das, «Identification of 38 keV γ Transition in ^{132}La Amidst X Rays», *Acta Phys. Pol. B* **50**, 173 (2019).

[40] S.P. Roberts *et al.*, «Low-spin studies of the $\pi h_{11/2}\nu h_{11/2}$ structure in ^{134}Pr», *Phys. Rev. C* **67**, 057301 (2003).

[41] S.V. Rigby *et al.*, «Decay of a $\pi h_{11/2} \otimes \nu h_{11/2}$ microsecond isomer in $^{136}_{61}\mathrm{Pm}_{75}$», *Phys. Rev. C* **78**, 034304 (2008).

[42] C.W. Beausang *et al.*, «Rotational band structures in doubly odd ^{138}Pm», *Phys. Rev. C* **42**, 541 (1990).

[43] J. Doring *et al.*, «In-beam study of excited states in ^{80}Br», *Z. Phys. A* **316**, 75 (1984).

[44] A.M. Bizzti-Sona *et al.*, «Yrast states in the doubly-odd nucleus ^{100}Tc», *Z. Phys. A* **352**, 247 (1995).

[45] A.M. Bizzti-Sona *et al.*, «The g factor of the lowest 7^+ state in ^{100}Rh and 6^- state in ^{104}Rh», *Z. Phys. A* **335**, 365 (1990).

[46] F.G. Kondev, G.D. Dracoulis, T. Kibédi, «Configurations and hindered decays of K isomers in deformed nuclei with $A > 100$», *At. Data Nucl. Data Tables* **103-104**, 50 (2015).

[47] P.M. Walker, S. Lalkovski, P.D. Stevenson, «Configuration dependence of K-forbidden transition rates from three-quasiparticle isomers», *Phys. Rev. C* **81**, 041304 (2010).

[48] P.M. Walker, «K-forbidden transitions in the N_pN_n scheme» *J. Phys. G: Nucl. Part. Phys.* **16**, L233 (1990).

[49] P.M. Walker, K. Schiffer, «Interpretation of $(h_{11/2})^2$ isomers in the $N \approx 76$ region of transitional nuclei», *Z. Phys. A* **338**, 239 (1991).

[50] P.M. Walker, «High-spin isomers: structure and applications», *Nucl. Phys. A* **834**, 22c (2010).

[51] T.P.D. Swan *et al.*, «Discovery of a nonyrast $K^\pi = 8^+$ isomer in ^{162}Dy, and the influence of competing K-mixing mechanisms on its highly forbidden decay», *Phys. Rev. C* **83**, 034322 (2011).

[52] P.M. Walker, «High-K isomers: some of the questions», *EPJ Web Conf.* **123**, 01001 (2016).

[53] P.M. Walker, «Isomer building blocks and K-forbidden decays», *Phys. Scr.* **92**, 054001 (2017).

[54] R.F. Casten, «A simple approach to nuclear transition regions», *Phys. Lett. B* **152**, 145 (1985).

[55] R.F. Casten, «Possible Unified Interpretation of Heavy Nuclei», *Phys. Rev. Lett.* **54**, 1991 (1985).

[56] R.F. Casten, N.V. Zamr, «Valence correlation schemes and signatures of nuclear structure: A simple global phenomenology for $B(\mathrm{E2}{:}2_1^+ \to 0_1^+)$ values», *Phys. Rev. Lett.* **70**, 402 (1993).

[57] P.M. Walker, P.D. Stevenson, «Configuration mixing and K-forbidden E2 decays», *Phys. Rev. C* **103**, 064305 (2021).